

Synaptic Facilitation in *Aplysia* Explored by Random Presynaptic Stimulation

JOHN P. KROEKER

From the Section of Neurobiology and Behavior, Division of Biological Sciences, Cornell University, Ithaca, New York 14853. Dr. Kroeker's present address is Bioinformation Systems, 286-80, California Institute of Technology, Pasadena, California 91125.

ABSTRACT The identified interneuron L10 in the abdominal ganglion of *Aplysia* was stimulated to fire action potentials in a random sequence while the early inhibitory potential of its follower cell L2 was recorded. Application of Wiener nonlinear analysis to these data yielded a predictive model of the facilitating postsynaptic potential. The model shows that facilitation changes both the time-course and the magnitude of the early synaptic potential. The facilitated response has a longer duration than the unfacilitated response. Its magnitude is exponentially decreasing with increasing interstimulus interval between test and conditioning stimuli. Facilitation is abolished at short interstimulus intervals. The hypothesis that the magnitude only of transmitter release is increased cannot explain these results. The observed facilitation may be due to characteristics of pre- and postsynaptic morphology.

INTRODUCTION

The generality of the Wiener method of nonlinear analysis makes it an attractive approach to an integrative neuronal model. In the context of synaptic function, this generality means the method can experimentally determine, and quantitatively describe, the modulation of synaptic response by any preceding pattern of activity. The Wiener description of a nonlinear synapse is obtained by cross-correlation of a random synaptic stimulus with the corresponding synaptic response, but it may be directly compared to models derived from double and multiple pulse experiments. The unique advantage of the Wiener method over deterministic stimulation is that it provides a measure of goodness-of-fit with respect to the entire galaxy of stimulus patterns present in the random stimulus. There is thus a measure of the applicability of the Wiener model to physiological reality that is lacking in models based on a small, predetermined class of stimuli.

The interneuron L10 (Frazier, et al., 1967) in the abdominal ganglion of *Aplysia californica* has cholinergic synapses on the cluster of large, bursting neurons L2-L6 (Pinsker and Kandel, 1969). The postsynaptic response of these bursting cells to an action potential in L10 is inhibitory, with three pharmacologically separable components (Kehoe and Ascher, 1970; Pinsker and Kandel, 1969). The earliest component of this response is due to an increase in chloride conductance and is easily inverted by postsynaptic hyperpolarization. The data

presented here show that the inverted early component of this synaptic response can demonstrate pronounced facilitation.

Quantitative models of synaptic facilitation have been developed to describe the change in magnitude of a facilitated response, depending on the lingering effects of previous action potentials (Linder, 1973; Magleby, 1973; Krausz and Friesen, 1977). Quantitative analysis of the facilitating early response of L2, however, demonstrates significant changes in the shape as well as the magnitude of the facilitated response. The data derived from Wiener analysis suggest that, at this synapse, a simple increase in the magnitude of transmitter release is insufficient to explain facilitation.

METHODS

Experimental

Aplysia californica (Pacific Biological Co., Richmond, Calif.) weighing 200–250 g were maintained before use without food in artificial seawater at 21°C. The abdominal ganglion was dissected out and pinned down under artificial seawater at 21°C. The ganglionic connective tissue sheath was dissected as necessary, and neurons L10 and L2 were impaled with glass microelectrodes (1–10 M Ω) filled with 3M KCL.

Cell L10 was simultaneously stimulated and monitored with a single microelectrode via a Wheatstone bridge. Depolarizing pulse stimuli of 6 ms duration, with 12 ms minimum interstimulus interval, were superimposed on a constant hyperpolarizing current stimulus. The pulse current, 5×10^{-7} A, was set such that L10 always fired an action potential after the pulse stimulus; the hyperpolarizing current, 2×10^{-8} A, was set such that L10 never fired spontaneously. The stimulus pulses were triggered by computer-generated pulses prerecorded on audio tape. The L10 membrane potential was AC-amplified and FM tape-recorded. Cell L2 was hyperpolarized with sufficient current, 2×10^{-8} A, to prevent firing under all stimulus conditions. Its potential was AC-amplified, with half-amplitude frequencies at 1 Hz and 1 KHz, and FM tape-recorded.

All data processing was done off-line with a PDP-8e (Digital Equipment Corp., Marlboro, Mass.) computer with a disk-operating system. Taped records of the L10 stimuli and the L2 response were digitized. The L2 response was low-pass filtered and sampled with 10 bits of resolution at 12 ms per sample. To prevent ringing after transients, a filter with a damped impulse response was used; frequency response was -3 dB at 120 Hz with 24 dB per octave roll-off. The number of stimuli to L10 that occurred during each of the L2 sampling periods was stored. The data presented here represent ~ 18 min of intracellular record, or 9.2×10^4 samples.

Design of the Random Stimulus

As discussed in the Appendix, for Wiener analysis of a system, the random stimulus applied to the system must generate all possible naturally occurring stimuli. The appropriate stimulus for systems with action-potential input is a modified Poisson process. A Poisson process of action potentials is defined by the requirements: first, that the probability of an action potential at any instant is constant over time; second, that this probability is independent of all previous action potentials. This stimulus must be modified to take into account the refractory period; two events in a Poisson process may occur arbitrarily close together, but two action potentials must be separated by a time at least as large as the refractory period.

In this experiment, a continuous-time random stimulus was approximated by generating action potentials on time-divisions 2 ms apart.

After each action potential, no new action potentials were allowed for 12 ms; thereafter, at each time-division the probability of generating an action potential was constant. Thus, allowable interstimulus intervals were 12, 14, 16, and so on. The stimulus mean frequency of 1.85/s was chosen to concentrate the patterns of action potentials generated by the random process in the physiological range.

Evaluation of the General Nonlinear Model

If a system's input and output are measured during consecutive intervals of time, then, for $i = 1, \dots, L$, x_i , and y_i will represent the measurements of the system input and output taken during the i th measurement interval. Here, y_i is a sample of a continuous output signal, and x_i is the count of the number of action potentials that occur in the i th interval. Because the sampling interval was chosen to equal the minimum interstimulus interval, x_i can only be one or zero.

Given a system with a memory of m measurement intervals, the output y_i may be predicted from the past input $x_{i-m}, x_{i-m+1}, \dots, x_i$ as follows. The Volterra functionals (see e.g., Deutsch, 1962) can be defined, for discrete measurements, by:

$$\begin{aligned} V_0(i) &= k_0, \\ V_1(i) &= \sum_{j=0}^m k_1(j)x_{i-j}, \\ V_2(i) &= \sum_{j=0}^m \sum_{k=0}^m k_2(j, k)x_{i-j}x_{i-k}, \end{aligned} \quad (1)$$

and in general by:

$$V_n(i) = \sum_{j_1=0}^m \dots \sum_{j_n=0}^m k_n(j_1, \dots, j_n)x_{i-j_1} \dots x_{i-j_n} \quad (2)$$

Each V_n is simply a polynomial of the x_i ; the k 's are the constant coefficients for each term of the polynomials. For instance, $k_1(2)$ is the coefficient for x_{i-2} . Because each x_i is either zero or one, terms in (2) of power greater than one can be neglected. For instance, in V_2 , the product $x_{i-j}x_{i-j} = x_{i-j}$, for x_{i-j} zero or one; thus $k_2(j, j)$ is a coefficient for a linear term; it can be absorbed into $k_1(j)$ and we can set $k_2(j, j) = 0$. Because $x_{i-j}x_{i-k} = x_{i-k}x_{i-j}$, we have $k_2(j, k) = k_2(k, j)$ and we need only evaluate $k_2(j, k)$ for $j < k$. Eq. 2 approaches the usual integral representation of the Volterra functionals as the intervals of the measurement get very small; the advantage of the discrete form is that it corresponds exactly to the measurement and computation procedures used in practice.

The system output y_i can be predicted by a sum of the V_n :

$$\hat{y}_i = V_0 + V_1(i) + V_2(i) + \dots + V_N(i), \quad (3)$$

where N is large enough to yield an accurate prediction.

The coefficients k_n of the model (Eq. 3) must be evaluated for a particular system, in order to predict the output of that system. The evaluation procedure is a two-step process. The coefficients of the Volterra model are not evaluated directly; to extract information efficiently about the system from the random stimulation data, the coefficients of the Wiener model, defined in the Appendix, are evaluated first. The coefficients of the Volterra model can then be determined by algebraic rearrangement of the Wiener coefficients.

For example, if the second-order model,

$$\hat{y}_i = V_0 + V_1(i) + V_2(i),$$

is to be evaluated, then the Wiener coefficients $f_0, f_1(j)$, and $f_2(j, k)$ are evaluated first.

The Wiener coefficients are found by cross-correlation of the output data with polynomials of the random input (Kroeker, 1977). If the input is a sequence of zeroes and ones, then the Wiener coefficients are given by Appendix Eq. A9:

$$f_0 = (L - m + 1)^{-1} \sum_{i=m}^L y_i,$$

$$f_1(j) = [(\lambda - \lambda^2)(L - m + 1)]^{-1} \sum_{i=m}^L y_i(x_{i-j} - \lambda),$$
(4)

and

$$f_2(j, k) = [2(\lambda - \lambda^2)^2(L - m + 1)]^{-1} \sum_{i=m}^L y_i(x_{i-j} - \lambda)(x_{i-k} - \lambda),$$

where λ is the mean number of action potentials per measurement of the stimulus; here $\lambda = 0.022$. The first m points of the output record are not included in the correlation, because for these points the past input to the system is not entirely known.

Given the Wiener coefficients and assuming a second-order system, the Volterra coefficients are given by Eqs. A8 and 1:

$$k_0 = f_0 - \lambda \sum_{j=0}^m f_1(j) + \lambda^2 \sum_{j=0}^m \sum_{k=0}^m f_2(j, k),$$

$$k_1(j) = f_1(j) - 2\lambda \sum_{k=0}^m f_2(j, k),$$
(5)

and

$$k_2(j, k) = f_2(j, k).$$

Computation Procedures

Eqs. 4 and 5 were implemented directly, in order to evaluate the coefficients of the Volterra functionals V_1 and V_2 . Inasmuch as the length L of the data record was very large, the sums required by Eq. 4 were normalized in segments, in order to maintain arithmetic accuracy. The mean of the stimulus was found by taking the mean over the experimental stimulus record.

As discussed in the Appendix, the refractory period of the action potential leads to small correlations between successive stimulus measurements, which can cause inaccuracies in the measurement of the f_n . In order to minimize these errors, as V_0 , V_1 , and V_2 were successively determined, the contributions of lower order models were subtracted from the output record prior to correlation. Thus, $y_i - V_0$ was correlated with x_i to yield the $k_1(j)$. Given $k_1(j)$, $V_1(i)$ can be computed. At this point the computations were checked by determining $k_1(j)$ for $y_i - V_0 - V_1(i)$; if the computations are correct, this must be zero. The record $y_i - V_0 - V_1(i)$ contains the information necessary to evaluate the $k_2(j, k)$; these coefficients were evaluated by cross-correlation of the difference record with the stimulus record, and the model V_2 was checked in the same way as V_1 .

If the f_n are evaluated correctly, they provide the best fit of a model of given order to the data. Any errors in the evaluation procedure will cause a deviation from this "best fit" property. The evaluation of the f_n was checked by computing the correlation between each model's output and its error. The error of a model is the difference between the output of the model and the system output. The coefficients that provide the best fit of a model to the data are found when the model output is independent of its error; the

Wiener technique is designed to have this property. The correlation between V_1 and its error was found to be 0.063; the correlation between $V_1 + V_2$ and its error was 0.060. Inasmuch as these correlations are both small, it is concluded that the coefficients found for these models provide a best-fit of the models to the data.

There is, as yet, no procedure for determination of the expected error of the values found for the Wiener coefficients, although upper bounds for the variance of Eq. 4 have been found (Kroeker, 1977; see also Marmarelis and Marmarelis, 1978). Therefore, three independent estimates of each point of the f_n were obtained as follows. The data records were segmented into three consecutive segments, each segment separated from the next by a gap of at least m measurements. Each correlation was performed for each of the three segments. Because the random stimulus has independent values at any two measurements that are not successive, the system output has independent values at instants that are more than $m + 1$ measurements apart, and therefore the three data segments are independent and the correlations performed on each are independent. The procedure also provides a control for drift in the system's properties; changing properties of the system will be reflected in differing values for the f_n for each data segment.

RESULTS

The first and second order Volterra models of the L2 synaptic response were evaluated according to Eqs. 4 and 5; cross-correlation of the digitized record of L2 potential with the record of L10 action-potential stimuli yielded the coefficients for these models. Because the DC component of the response was not recorded, the DC component of the Volterra model, V_0 , is set to zero; thus, the first order Volterra model of the recorded response is given (Eq. 3) by V_1 alone. The coefficients of V_1 , as evaluated by the Wiener method, produce the best mean-square fit of the model to the response data. The model V_1 accounts for 83.8% of the response variance with these coefficients. The best-fitting coefficients of the second order Volterra model $V_1 + V_2$ were also evaluated; the second order model accounted for an additional 4.4% of the response variance. Note that V_1 is revised according to Eq. 5 in the second order model; from now on, V_1 will refer only to this revised version. Analysis of the L2 potential, observed after cessation of L10 stimulation, indicated that 1.1% of the response variance was due to noise unrelated to the L10 stimulus. Thus, 10.7% of the variance remains unexplained.

The recorded postsynaptic response of L2 to an L10 action potential consists of an initial depolarization followed by a smaller hyperpolarization, as illustrated in Fig. 1 A. As shown in Fig. 1 B, the V_1 component of the second order model roughly predicts the observed response to a single action potential; the entire second order model $V_1 + V_2$ does not improve upon this prediction. The postsynaptic response to multiple action potentials is not predicted by V_1 alone. Fig. 1 B demonstrates the discrepancy between the response of V_1 to a high-frequency burst of three stimuli and the L2 response to the same stimuli. This discrepancy indicates clearly that the L2 response facilitates with high-frequency stimulation; facilitation is an excess of response over that predicted by a summated single-stimulus. The model $V_1 + V_2$ yields a much better prediction of the L2 response to high-frequency stimuli; note that the peak L2 response in Fig. 1 B is more closely approached by $V_1 + V_2$ than by V_1 alone.

The coefficients $k_1(j)$ of V_1 correspond to the model response to a single action potential; if the model receives a single stimulus at time zero, then the magnitude of the model response at time j is $k_1(j)$. The passive cable equation for an infinite cylindrical membrane was fit to $k_1(j)$. For an instantaneous current applied a distance x from the recording electrode, the recorded potential $V(t)$ at time t is (Jack et al., 1975):

$$V(t) = AT^{-3/2} \exp(-B/T - T), \quad (6)$$

where $T = t/\tau - \delta$, $B = x^2/2\lambda^2$, and $A = Q_0(2c_m\lambda\sqrt{\pi})^{-1}$. Here, τ is the membrane time constant, λ is the length constant, δ is the (normalized) time of application

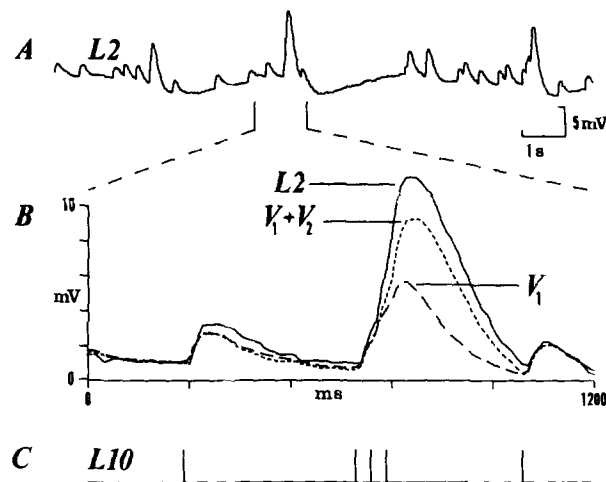


FIGURE 1. Comparison of the L2 synaptic response to the second order Volterra model. (A) 1,024-point sample, 12 ms/point, of the digitized record of the L2 response to random stimulation of L10. Upward deflections are the early inhibitory synaptic responses, inverted by postsynaptic hyperpolarization. (B) An expansion of the indicated portion of A is given by the solid line. The corresponding L10 action-potential stimuli are represented by the vertical ticks in C. The dotted line shows the responses, to the same stimuli, of the entire second-order Volterra model, $V_1 + V_2$. The dashed line shows the V_1 component alone. The V_1 response to a single stimulus is close to the L2 response, but the linear summation of single-stimulus responses, predicted by V_1 , fails to match the L2 response to multiple stimuli. The $V_1 + V_2$ response is closer to the facilitated, multiple-stimulus response of L2.

of the stimulus current, Q_0 is the amount of charge applied, and c_m is the membrane capacitance. The parameters A , B , δ , and τ , were varied according to the method of steepest descent (see e.g., Bevington, 1969) to obtain the best least squares fit of Eq. 6 to the first 16 points of $k_1(j)$. The resulting equation is, for t in milliseconds and V in millivolts:

$$V(t) = 10.3T^{-1/2} \exp(-0.821/T - T), \quad (7)$$

where $T = t/97.5 + 0.941$. The value of B corresponds to a presumed electrotonic distance from stimulus to electrode of 1.28 length constants.

The $k_1(j)$ were determined for each of the three independent segments of the random-stimulation data. The k_1 found for the entire record, the range of values found for the three determinations of k_1 , and the best-fitting cylindrical cable equation (Eq. 7) are shown in Fig. 2.

The coefficients $k_2(j, k)$ of V_2 describe the change in a system's response due to system properties that depend on two stimuli. That is, because $k_2(j, j) = 0$, V_2 contributes nothing to the model response to a single stimulus, but if there are two stimuli at times $i - j$ and $i - k$, then V_2 contributes an amount $k_2(j, k)$, to be added at time i , to the response of the model $V_1 + V_2$. The separation between the two stimuli is $s = j - k$; if a stimulus is presented at time zero is preceded by another stimulus, and if the separation between the two stimuli is s , then at time

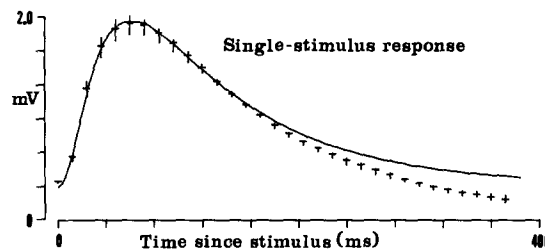


FIGURE 2. The coefficients $k_1(j)$ for the Volterra functional V_1 . The $k_1(j)$, for $j = 1-32$, represent the single-stimulus response, specified at 12-ms intervals, of the second-order Volterra model. The vertical bars indicate the range of variation for each coefficient, for the coefficients separately determined from three independent segments of the random-stimulation data. The intersections of the vertical and horizontal bars give the values of the $k_1(j)$ determined from the entire data record. The solid line gives the values of the passive cable equation for an infinite cylinder (Eq. 7), best-fit to the first 16 coefficients.

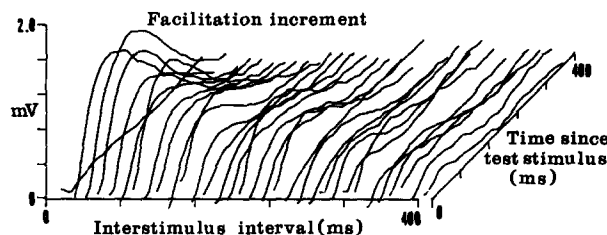


FIGURE 3. The facilitation increments F_s . The $F_s(j)$, $s = 1-32$, from left to right, are shown in isometric projection. The values of each $F_s(j)$, for $j = 1-32$, are connected by a continuous line. The F_s represent the response contributed by V_2 of the second-order model $V_1 + V_2$. The interval between a conditioning and a test stimulus, for each $F_s(j)$, is $12 \cdot s$ ms and is given by the horizontal axis. The time after the test stimulus is $12 \cdot j$ ms and is given by the slanted axis. Each F_s gives the extra amount to be added to the test response, due to the facilitating effects of a conditioning stimulus s measurement intervals in the past.

j , V_2 contributes $k_2(j, j + s)$ to the model output. Thus, for each s , a facilitation increment function F_s can be defined by:

$$F_s(j) = k_2(j, j + s). \quad (8)$$

F_s is the function of time that is added to the postsynaptic response to a test action potential that is separated from a preceding conditioning action potential by s measurement intervals. The F_s , for all s , embody all the information contained in the coefficients $k_2(j, k)$; they are the diagonals of the matrix with elements $k_2(j, k)$. Fig. 3 shows an isometric projection of the F_s . Facilitation can be seen to be strongest at a stimulus separation of 36 ms and to become progressively smaller with increasing or decreasing stimulus separation.

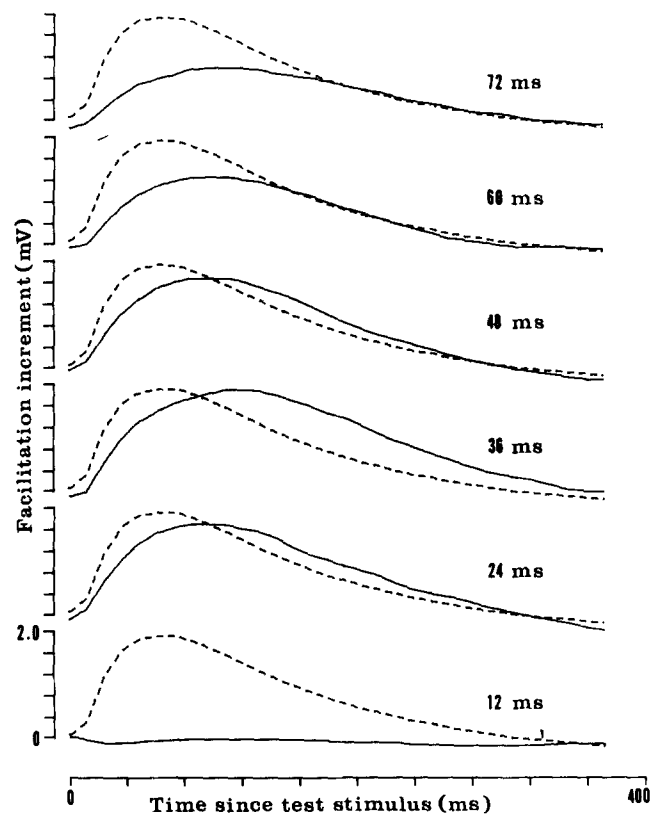


FIGURE 4. The facilitation increment functions $F_1(j)$ through $F_6(j)$. The values of each $F_s(j)$, for $j = 1-32$, are connected by a continuous line. For comparison, the unfacilitated, single-stimulus response is given by the dashed line in each graph of F_s . The graphs are all to the same scale. The interstimulus interval, $12 \cdot s$ ms, is given for each F_s . The time, $12 \cdot j$ ms, after the test stimulus, is given by the horizontal axes. At a 12-ms interstimulus interval, the facilitation increment F_1 is essentially zero, but at 24 ms, the facilitation increment is large; maximum facilitation occurs at a 36-ms interstimulus interval. The half-widths of the F_s shown here range from 30-60 ms larger than the 140-ms half-width of the single-stimulus response.

Fig. 4 shows the first six F_s in greater detail; for comparison, k_1 is indicated by the dotted line on each graph of F_s . At a separation of 12 ms, the facilitation-increment function, given by F_1 , is zero; at a separation of 36 ms, the facilitation increment is largest and longest lasting. Note that at a 36-ms separation, the peak facilitation increment is larger than k_1 ; the response to a second stimulus, at this separation, is approximately doubled due to facilitation. At separations

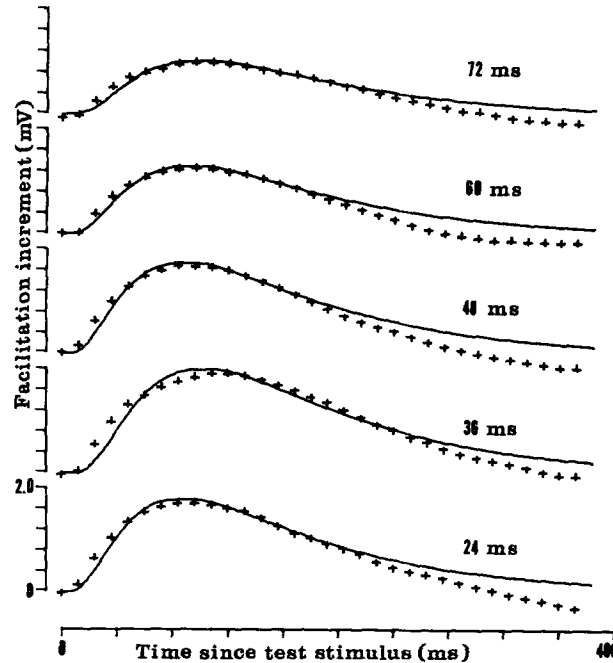


FIGURE 5. F_2 through F_6 compared to the best-fitting cable equation. The passive cable equation for an infinite cylindrical membrane was fit to the first 16 points of each F_s , with the membrane time constant fixed at the value obtained from $k_1(j)$. The values of the $F_s(j)$ are given by crosses. The values of the best-fitting cable equation, for each F_s , are given by the continuous lines. Scales as in Fig. 4.

of 24–48 ms, F_s is clearly broader than the single-stimulus response; this effect is confirmed by comparison of the half-widths of F_s and k_1 . The small signal-to-noise ratio of F_s , for large s , precludes accurate measurement of the half-widths of these F_s . The half-widths of F_2 through F_5 , however, were consistently larger than the half-width of k_1 ; they varied from 30 to 60 ms larger than the 140-ms half-width of k_1 , being largest for F_3 .

In order to examine the hypothesis that the F_s represent a physiologically additive input, the cable equation (Eq. 6) was fitted to each of the F_s . As the system time constant must be the same for all additive inputs to a passive membrane system, τ in Eq. 6 was constrained to have the value determined for k_1 . The best-fitting curves for F_s , $s = 2-6$, are compared to the F_s in Fig. 5. The average of the parameter δ , for $s = 2-31$, is -2.64 ms; it ranges from -6.12 to

0.20 ms for the first 16 F_s , increasing further in variability for the last 16 F_s . The electrotonic distance derived from the average of $B(2)$ to $B(31)$ is 1.90 length constants, ranging from 1.23 to 2.44 for the first 16 F_s and increasing in variability for the last 16 F_s .

The hypothesis that increased response duration during facilitation is caused by increased duration of synaptic current was also examined by curve-fitting. The parameters δ , λ , and τ found for k_1 were held constant, and Eq. 6 was numerically integrated to find the predicted response to a current pulse. The duration of the current was varied to yield the best fit to the first 16 points of the entire facilitated response, $k_1 + F_s$. The average duration of current for the first 16 facilitated responses is 26.0 ms, ranging from 21 to 34 ms. The cylindrical cable equation with a pulse input fits the first 16 points of the facilitated response as well as does the cable equation with an additive input.

Fig. 6 shows the peak magnitudes of the F_s plotted on a logarithmic scale. A linear regression of the log of peak magnitude on s , for $s = 2-31$, predicts peak magnitude $p(t)$ as a function of stimulus separation time by: $p(t) = 1.83 \exp(-t/165)$, where $p(t)$ is in millivolts and t is in milliseconds; $t = 12s$.

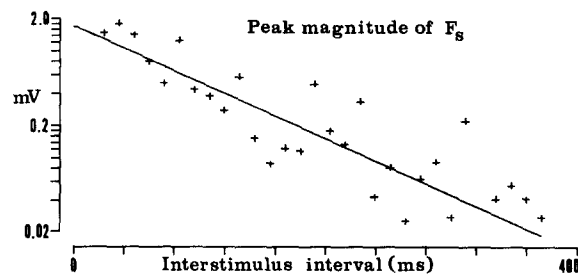


FIGURE 6. Log of peak magnitude of the facilitation increments. The logarithm of the peak magnitude of each F_s , $s = 2$ through 31, is graphed against the interstimulus interval, given by $12 \cdot s$ ms, and compared to the regression line for $\log(F_s)$ vs. s . Decay of peak magnitude is roughly exponential with increasing interstimulus interval. The value of F_{25} is nearly two orders of magnitude below the other points and is not included on this graph, although it was included in the regression.

The F_s were also determined separately for each of the three independent segments of the random-stimulation data. The range of variation of F_s is much larger than that of k_1 , being of the same magnitude as the F_s themselves. The F_s did not change consistently over the three segments of data; thus, facilitation exhibits no long-term drift. The qualitative relations between k_1 and F_s were the same for each segment as those reported here for the entire record.

DISCUSSION

The Early Component of the L2 Synaptic Response Facilitates

The second order Volterra model predicts the facilitation of the early, experimentally inverted, component of the L2 response to an L10 action potential.

This model describes facilitation of the L2 response as follows. Suppose two action potentials are elicited in L10, a test action potential preceded by a conditioning action potential. Each stimulus action potential, if applied separately, would produce the unfacilitated response k_1 shown in Fig. 2. Were facilitation absent, the response to the stimuli applied together would be the sum of these separate responses. The actual facilitated response is given by this sum plus an additional response to the test action potential; the extra response depends on the separation between conditioning and test action potentials and is called here the facilitation-increment function F_s , where s is the number of intervals between two stimuli. The model predicts the facilitation increment of a test stimulus preceded by n conditioning stimuli by the sum of n facilitation increments F_s , one for each conditioning stimulus.

Wiener evaluation of the coefficients of the Volterra model produces a model of the synaptic response that is the best predictor of the response to the collection of stimulus patterns present in the random stimulus. However, the Volterra model of a system makes no assumptions about the internal structure of the system, nor does it necessarily provide any information about that internal structure. Although an accurate model of the neuron need not reflect the internal structure of the neuron to be of use in modelling the behavior of an assemblage of neurons, the model neuron should nevertheless be susceptible of physiological interpretation.

The interneuron L10 has been shown to make an inhibitory monosynaptic connection with L2 (Pinsker and Kandel, 1969); there are three components of the response of this synapse (Kehoe and Ascher, 1970; Kehoe, 1972). The early synaptic response is due to a chloride permeability change induced by a D-tubocurarine-sensitive cholinergic receptor. This response is independent of a second component produced by a potassium current that is induced by a methylxylcholine-sensitive cholinergic receptor; it is also independent of the long-lasting, possibly electrotonic, inhibition at this synapse.

This information has been obtained with the use of action-potential bursts as the synaptic stimulus; stimulation frequencies of 10/s and 15/s have been indicated (Pinsker and Kandel, 1969; Kehoe and Ascher, 1970). The Volterra model response to 2-s bursts of stimuli showed that, at a frequency of 10.4/s, the predicted facilitation is responsible for an increase of 60% in the peak magnitude of the response; at 27.8/s, facilitation increases the model response by 350%. Thus, the Volterra model predicts that both the single-stimulus and the facilitation components of the early response are elicited in response to L10 action potential bursts. If so, it follows that both components are due to a D-tubocurarine-sensitive cholinergic receptor that increases the chloride permeability of L2.

The long-lasting inhibitory components of the L2 response, although filtered out of the L2 data record, must nonetheless cause long-lasting changes in the membrane potential of L2, depending on the long-term changes in activity of the random stimulus. This variation in membrane potential must cause corresponding variation in the magnitude of the early chloride potential; the magnitude of the chloride potential varies directly as the difference of the membrane potential and the chloride equilibrium potential. This effect may

account for the variance of the L2 record that is unexplained by the second-order model; a third-order model would be required to predict facilitation while taking into account the effects of stimuli far in the past. The second-order model must predict a response which is sometimes too large and sometimes too small to produce the best fit to the entire data record; the sample of the model response shown in Fig. 1 is too small, whereas in other portions of the model-response record it was too large.

A Scalar Increase in Transmitter Release Cannot Explain Facilitation

Facilitation at individual neuromuscular junctions has been shown to result from an increase in the amount of transmitter released from the presynaptic terminals in response to a given depolarization (del Castillo and Katz, 1954; Rahamimoff, 1968). In this case, the facilitated response is caused by a scalar increase in the release of transmitter; the time-course of release remains unchanged. The facilitation-increment functions F_2 through F_{31} demonstrate that facilitation at the L2-L10 synapse, when it occurs, is associated with an increase in the half-width of the postsynaptic response. If facilitation were caused by an increase in the magnitude of transmitter release, with no change in the time-course of release, then, assuming linearity of the postsynaptic membrane, the postsynaptic potential would increase in magnitude, but not in half-width. Simple variation in the magnitude of transmitter release is therefore insufficient to explain facilitation at this synapse.

Facilitation May Be Modulated by Morphology

The facilitated postsynaptic potential could increase in duration by several mechanisms; the time constant of the postsynaptic cell could be altered, the duration of postsynaptic current could be increased, or current could be injected at a greater distance from the postsynaptic soma. The physiological characteristics required for each of these possibilities to explain the increase in duration of the facilitated response can be indicated by the best-fitting cable equation for an infinite cylindrical membrane. Although this equation is based on a gross oversimplification of the postsynaptic morphology, it yields a surprisingly good first approximation to the data and is useful as a convenient point of reference. The cable equation indicates, for instance, that the duration of postsynaptic current must be increased ~ 26 ms to account for the facilitated response. On the other hand, if facilitation involves a second current source at some greater distance from the recording electrode, the cable equation indicates that the second source must be ~ 0.6 length constants more distant.

The high-frequency failure of facilitation may yield a clue to the mechanism responsible for the increase in duration of the facilitated response. Facilitation is strong at an interspike interval of 24 ms, but entirely absent at an interspike interval of 12 ms. This failure of the facilitation component of the response suggests a failure of the presynaptic action potential due to the refractory period of the preceding action potential. That only the facilitation component is subject to this failure, whereas the unfacilitated response k_1 is always maintained, suggests that facilitation may be mediated by a second axon branch with a longer refractory period. Such an increase in the refractory period could be due

to a sudden enlargement of diameter, such as a branch point (Parnas et al., 1976; Yau, 1976).

Although neither the hypothesis of increased time constant nor increased duration of current is ruled out, the possibility that the increased duration of facilitation is due to postsynaptic separation of current sources is attractive. The existence of two components of the synaptic response, indicated by high-frequency failure of facilitation, also explains the increased duration of facilitation if these components are postsynaptically spatially separated. These separated components may well correspond to the two distinct regions of dendritic branching in L2 demonstrated by cobalt injections of this neuron (Winlow and Kandel, 1976).

APPENDIX

Wiener Analysis with a Random Action-Potential Stimulus

1. *The Random Action-Potential Stimulus*

Suppose a random process is measured on m non-overlapping intervals of time, I_i , $i = 1, \dots, m$, and that the observed value of the process on each interval is x_i . The fundamental requirements for the random stimulus are (a) x_i must be mutually independent random variables; and (b) each measurement x_i must have nonzero probability of taking on any value that could occur in a natural stimulus. If (a) and (b) hold for all collections of measurements, then these requirements become quite stringent.

If a random stimulus satisfies (a) and (b), any possible sequence of measurements x_1, x_2, \dots, x_m has nonzero probability of occurring. It follows, for a sufficiently long application of the stimulus, that all possible sequences of measurements will occur, and the stimulus will exhaustively test the unknown system with all possible inputs. If the system normally receives a series of identical events as input, then (a) and (b) lead to the use of the Poisson process as the random stimulus. Wiener analysis of neural systems that receive as input a series of identical action potentials could therefore use a Poisson process of action potentials as a random stimulus.

Because of the refractory period of the action potential, a true Poisson process of action potentials cannot be physically generated. Instead, the Poisson process with dead time must be used, where the dead time d is the period of time after each event during which no new events are allowed to occur (Haight, 1967). If the dead time equals the absolute refractory period of the action potential, then all possible natural stimuli will still be produced. However, because the dead time may straddle two adjacent intervals of measurement, property (a) is not always satisfied, and therefore the Wiener analysis technique, in its current form, must be approximated.

Consider the situation where the intervals of measurement are no larger than d ; this is not a theoretically limiting restriction. In this case, the maximum number of events that can be measured in any one interval is one, and the measurement is therefore a Bernoulli random variable with value either zero or one. Given this restriction, there are two ways of proceeding.

The first method, due to Craig¹ (Craig and Tapper, 1977), sacrifices the generality of the random stimulus, in order to maintain the generality of the Wiener analysis procedure. Independent stimulus events are produced only at times that are multiples of

¹ Craig, A. D., Jr. Personal communication.

the dead time. If the measurement intervals are of duration d and each begin at one of the allowed stimulation times, then the dead time of the stimulus always falls entirely within a single measurement interval. In this case, measurements of the random stimulus made during different intervals will always be independent, satisfying requirement (a). This method does not test all possible input functions, because of the restriction of stimulus times, but it has the advantage that the procedure presented in the next section may be applied in a straightforward and rigorous manner.

The second method, used here, maintains the generality of the random stimulus, but sacrifices the generality of the Wiener analysis procedure. The Poisson process with dead time is used as the stimulus, and the stimulus is measured with intervals of duration d , so that at most one event is measured in each interval. This method has the advantage that the system is analyzed with a random stimulus that applies the complete class of possible inputs. However, the method can only be used with a low mean frequency of stimulus events, and the method is not applicable to all classes of systems.

In particular, this method results in measurements of the random stimulus that are correlated. Suppose that the probability that $x_i = 1$ can be predicted given knowledge of x_{i-1} . Thus, given $x_{i-1} = 0$, there is probability λ that $x_i = 1$, but given $x_{i-1} = 1$, if the time of occurrence of the event within I_{i-1} has the uniform distribution, then the probability that $x_i = 1$ is reduced to $1/2\lambda$. In this case, the measurements x_1, \dots, x_m are a sample of a two-state Markov chain. This type of random process has been well analyzed (Feller, 1968), and it can be shown that the serial correlation coefficient ρ_n , between two measurements m intervals apart, is:

$$\rho_n = (-1/2\lambda)^n. \quad (\text{A1})$$

Thus, for λ small, the correlation between measurements is small, and requirement (a) is approximately satisfied. In this experiment, the serial correlations were found to agree with Eq. A1, with a maximum value at $\rho_1 = -0.011$. The actual errors introduced to the Wiener analysis by these correlations will depend on the magnitude of each component of the Wiener expansion, and the validity of the Wiener analysis must be empirically verified for each system.

2. The Bernoulli-Wiener Expansion

The x_i are assumed to be independent Bernoulli variables; that is, each x_i is independent of x_j , for $j \neq i$; $x_i = 1$ with probability λ ; and $x_i = 0$ with probability $1 - \lambda$. Under these assumptions, Craig's¹ formulation of the Wiener cross-correlation procedure for a Bernoulli stimulus will now be developed in its general setting. See McCann and Marmarelis (1975) and Marmarelis and Marmarelis (1978) for other approaches. We wish to represent any function of x_1, \dots, x_m by a linear combination of orthogonal polynomials of the x_i . These polynomials can be developed exactly like the Poisson-Charlier polynomials (Kroeker, 1977); I shall only point out the major differences here.

Any function f of one Bernoulli variable can only have two values, $f(0)$ and $f(1)$; it follows that f can always be represented by a constant and a linear term. Therefore, any such f can be represented by a linear combination of the trivial set of polynomials:

$$\begin{aligned} b_0(x) &= 1, \\ b_1(x) &= x - \lambda, \end{aligned}$$

and

$$b_n(x) = 0, \quad (\text{A2})$$

for $n > 1$. The b_n , $n > 1$, have mean zero. They are orthogonal in the sense that the

(mean) product of any two different b_n is zero; indeed, this follows from the fact that the expectation of $b_0 b_1$ is zero. The expectation of b_1^2 is $\lambda - \lambda^2$.

Polynomials of n Bernoulli variables x_{i_1}, \dots, x_{i_n} chosen from the collection x_1, \dots, x_m can be defined by:

$$\begin{aligned} b^n(x_{i_1}, \dots, x_{i_n}) &= b_1(x_{i_1}) \cdot \dots \cdot b_1(x_{i_n}) \\ &= (x_{i_1} - \lambda) \cdot \dots \cdot (x_{i_n} - \lambda), \end{aligned} \quad (\text{A3})$$

for i_1, \dots, i_n all different; b^n is zero otherwise.

The b^n polynomials have all the properties of the Poisson-Charlier polynomials (Kroeker, 1977). In particular, $E b^n = 0$, where E denotes the expectation with respect to the multivariate Bernoulli distribution. Furthermore, if x_{i_1}, \dots, x_{i_n} and x_{j_1}, \dots, x_{j_k} are two different selections of variables from x_1, \dots, x_m , then

$$E b^n(x_{i_1}, \dots, x_{i_n}) b^k(x_{j_1}, \dots, x_{j_k}) = (\lambda - \lambda^2)^n, \quad (\text{A4})$$

if some permutation of i_1, \dots, i_n matches j_1, \dots, j_k ; Eq. A4 is zero otherwise.

The Bernoulli-Wiener functional is defined by:

$$J_n(i) = \sum_{j_1=1}^m \dots \sum_{j_n=1}^m f_n(j_1, \dots, j_n) b^n(x_{i-j_1}, \dots, x_{i-j_n}), \quad (\text{A5})$$

where the f_n are constant coefficients for each choice of i_1, \dots, i_n .

The Bernoulli-Wiener model of a system is:

$$\hat{y}_i = \sum_{n=0}^N J_n(i), \quad (\text{A6})$$

where \hat{y}_i is the predicted output of the system at time i , and N is sufficiently large to yield a good prediction of the actual system output y_i . For example, the second order Bernoulli-Wiener model is:

$$\hat{y}_i = J_0 + J_1 + J_2, \quad (\text{A7})$$

where

$$\begin{aligned} J_0 &= f_0 \\ J_1(i) &= \sum_{j=0}^m f_1(j) (x_{i-j} - \lambda), \\ J_2(i) &= \sum_{j=0}^m \sum_{k=0}^m f_2(j, k) (x_{i-j} - \lambda) (x_{i-k} - \lambda). \end{aligned} \quad (\text{A8})$$

The model (Eq. A6) is evaluated for a particular system by determining the coefficients f_n . These coefficients need only be evaluated for values of the indices j_1, \dots, j_n in Eq. A5, that are all different.

The J_n functionals have all the properties of the Poisson-Charlier functionals (Kroeker, 1977); in particular, the coefficients in Eq. A5 may be found by cross-correlation of the data from the random-stimulus experiment. For stationary systems, systems whose properties don't change over time, the experimental estimate of each $f_n(j_1, \dots, j_n)$ is computed by:

$$\overline{f_n(j_1, \dots, j_n)} = [n! (\lambda - \lambda^2)^n]^{-1} \overline{y_i(x_{i-j_1} - \lambda) \cdot \dots \cdot (x_{i-j_n} - \lambda)}, \quad (\text{A9})$$

where the overbar indicates time average. Given the random-stimulus experiment data, Eq. A9 yields the best possible estimate of the f_n . The evaluation-relation Eq. A9 differs

from that of the Poisson-Charlier expansion only in the substitution of $(\lambda - \lambda^2)^n$ for λ^n as a normalizing factor.

I would like to thank B. P. Halpern for constant encouragement and support and A. D. Craig, Jr. for many valuable suggestions.

This work was supported in part by grant BNS 74-00878 from the National Science Foundation and the Cornell University Office of Academic Funding.

Received for publication 3 August 1978.

REFERENCES

- BEVINGTON, P. R. 1969. *Data Reduction and Error Analysis for the Physical Sciences*. McGraw-Hill Book Company, New York. 336 pp.
- CRAIG, A. D., JR., and D. N. TAPPER. 1977. Nonlinear analysis of dorsal horn cells. *Neuroscience*. **3**:500.(Abstr.)
- DEL CASTILLO, J., and B. KATZ. 1954. Statistical factors involved in neuromuscular facilitation and depression. *J. Physiol. (Lond.)*. **124**:574-585.
- DEUTSCH, R. 1962. *Nonlinear Transformations of Random Processes*. Prentice-Hall, Inc., Englewood Cliffs, N.J. 157 pp.
- FELLER, W. 1962. *An Introduction to Probability Theory and its Applications*. 3rd edition, Vol. I. John Wiley & Sons, Inc., New York. 509 pp.
- FRAZIER, W. T., E. R. KANDEL, I. KUPFERMANN, R. WAZIRI, and R. E. COGGESHALL. 1967. Morphological and functional properties of identified neurons in the abdominal ganglion of *Aplysia californica*. *J. Neurophysiol.* **30**:1288-1351.
- HAIGHT, F. A. 1967. *Handbook of the Poisson Distribution*. Publications in Operations Research, No. 11. Operations Research Society of America. John Wiley & Sons, Inc., New York. 168 pp.
- JACK, J. J. B., D. NOBLE, and R. W. TSIEN. 1975. *Electric Current Flow in Excitable Cells*. Clarendon, Oxford. 502 pp.
- KEHOE, J. S. 1972. The physiological role of three acetylcholine receptors in synaptic transmission in *Aplysia*. *J. Physiol. (Lond.)*. **225**:147-172.
- KEHOE, J. S., and P. ASCHER. 1970. Re-evaluation of the synaptic activation of an electrogenic sodium pump. *Nature (Lond.)*. **225**:820-823.
- KRAUSZ, H. I., and W. O. FRIESEN. 1977. The analysis of nonlinear synaptic transmission. *J. Gen. Physiol.* **70**:243-265.
- KROEKER, J. P. 1977. Wiener analysis of nonlinear systems using Poisson-Charlier crosscorrelation. *Biol. Cybern.* **27**:221-227.
- LINDER, T. M. 1973. Calcium and facilitation at two classes of crustacean neuromuscular synapses. *J. Gen. Physiol.* **61**:56-73.
- MAGLEBY, K. L. 1973. The effect of repetitive stimulation on facilitation of transmitter release at the frog neuromuscular junction. *J. Physiol. (Lond.)*. **234**:327-352.
- MARMARELIS, P. Z., and V. Z. MARMARELIS. 1978. *Analysis of Physiological Systems*. Plenum, N.Y. 500 pp.
- MCCANN, G. D., and P. Z. MARMARELIS. 1975. *Proceedings of the First Symposium on Testing and Identification of Nonlinear Systems*. California Institute of Technology, Pasadena, Calif. 383 pp.
- PARNAS, I., S. HOCHSTEIN, and H. PARNAS. 1976. Theoretical analysis of parameters leading to frequency modulation along an inhomogeneous axon. *J. Neurophysiol.* **39**:909-923.

KROEKER *Facilitation in Aplysia*

763

PINSKER, H., and E. R. KANDEL. 1969. Synaptic activation of an electrogenic sodium pump. *Science (Wash. D. C.)*. **163**:931-935.

RAHAMIMOFF, R. 1968. A dual effect of calcium ions on neuromuscular facilitation. *J. Physiol. (Lond.)*. **195**:471-480.

WINLOW, W., and E. R. KANDEL. 1976. The morphology of identified neurons in the abdominal ganglion of *Aplysia californica*. *Brain Res.* **112**:221-249.

YAU, K-W. 1976. Receptive fields, geometry and conduction block of sensory neurones in the central nervous system of the leech. *J. Physiol. (Lond.)*. **263**:513-538.